

# Representation Learning on Variable Length and Incomplete Wearable-Sensory Time Series

Xian Wu, Chao Huang, Pablo Roblesgranda, Nitesh Chawla

University of Notre Dame  
{xwu9, chuang7, problesg, nchawla}@nd.edu

## Abstract

The prevalence of wearable sensors (*e.g.*, smart wristband) is enabling an unprecedented opportunity to not only inform health and wellness states of individuals, but also assess and infer demographic information and personality. This can allow us a deeper personalized insight beyond how many steps we took or what is our heart rate. However, before we can achieve this goal of personalized insight about an individual, we have to resolve a number of shortcomings: 1) wearable-sensory time series is often of variable-length and incomplete due to different data collection periods (*e.g.*, wearing behavior varies by person); 2) inter-individual variability to external factors like stress and environment. This paper addresses these challenges and brings us closer to the potential of personalized insights whether about health or personality or job performance about an individual by developing a novel representation learning algorithm, *HeartSpace*. Specifically, *HeartSpace* is capable of encoding time series data with variable-length and missing values via the integration of a time series encoding module and a pattern aggregation network. Additionally, *HeartSpace* implements a Siamese-triplet network to optimize representations by jointly capturing intra- and inter-series correlations during the embedding learning process. Our empirical evaluation over two different data presents significant performance gains over state-of-the-art baselines in a variety of applications, including personality prediction, demographics inference, user identification.

## Introduction

The wide proliferation of wearables and mobile devices is revolutionizing health and wellness with the potential of data and personalized insights at one’s fingertips (Op De Beéck, Meert, and others 2018). These wearables generate chronologically ordered streams (*e.g.*, the series of heart rate measurements), which provide an unprecedented opportunity to learn about health and wellness states, as well as how those interact with the social network, opinions and personality. To better analysis wearable-sensory time series data for their perceived benefit for a wide spectrum of applications, the fundamental question is: how do we effectively featurize the

wearable-sensory time series data, while achieving the generalization purpose for a multitude of applications?

A body of time series analysis has focused on wavelet-based frequency analysis (Sun, Leng, and etc 2015) and motif discovery methods (Zhu et al. 2018). But, these methods carry their own limitations. First, while we can extract discriminating and independent features using wavelet decomposition approaches, it still involves manual effort and domain-specific knowledge (*e.g.*, medical knowledge) (Bai et al. 2018). Second, discovering motifs are computationally expensive and require the repeated process of searching for optimal motifs from candidates (Liu et al. 2015).

Motivated by these limitations and the success of representation learning, recent research has led to representation learning on sensory data (Ballinger et al. 2018; Wang et al. 2018; Ni, Muhlstein, and McAuley 2019). However, these works have focused on representation learning for fixed-length sequential data with high quality complete time series data and face their own set of limitations. *First*, the wearable-sensory time series data is of variable-length and incomplete ranging from several days to months, since the actively sensing time period may vary from person to person (Liu et al. 2016; Manashty, Light, and Soleimani 2018). *Second*, there are localized patterns among individuals (intra-sensor / individual variability) that offer important nuances on similarities and differences. They fail to preserve the local characteristics of such time series data in representation learning.

To overcome the above limitations, we propose a novel and effective framework, *HeartSpace*, to learn a generalizable lower-dimensional and latent representation of wearable-sensory time series. Building upon the unsupervised learning paradigm, in *HeartSpace*, we first segment the heart rate data collected from individuals into multiple day-long time series variable-length time series because human behavior exhibits day-long regularities. Then, a deep autoencoder architecture is developed to map high-dimensional time-specific (*i.e.*, daily) sensor data into the common latent space, with a dual-stage gating mechanism to handle variable-length time series. These learned embedding vectors are capable of not only preserving temporal variation patterns, but also largely alleviating the data missing

issue of wearable-sensory time series. After that, we leverage a temporal pattern aggregation network to capture inter-dependencies across time-specific representations based on the developed position-aware multi-head attention mechanism. During the training process, a Siamese-triplet network optimization strategy is designed with the exploration of implicit intra-series temporal consistency and inter-series relations. To summarize, our main contributions are as follows:

- We perform comprehensive study on addressing challenges of learning representations on variable length and incomplete wearable time series data.
- We develop a novel and effective unsupervised learning framework, *HeartSpace*, to learn a generalizable low-dimensional and latent embedding by aggregating variable-length time series and capturing their intra-series and inter-series relations. *HeartSpace* is also flexible to be generalized into semi-supervised learning for various heart rate analysis application.
- We evaluate *HeartSpace* on three learning tasks with two real-world wearable-sensory time series datasets, and the experiments demonstrate the effectiveness of *HeartSpace*.

## Problem Formulation

In this section, we introduce key preliminary definitions and formalize the studied problem.

**Definition 1 Wearable-Sensory Time Series.** Suppose there are  $I$  users ( $\mathcal{U} = \{u_1, \dots, u_I\}$ ), we use  $\mathbf{x}_i = (x_{i,1}, \dots, x_{i,J_i})$  ( $\mathbf{x}_i \in \mathbb{R}^{J_i}$ ) to denote the series of temporally ordered wearable-sensory data (e.g., heart rate measurement—the number of times a person’s heart beats per minute) of length  $J_i$  collected from user  $u_i$ . In particular, each element  $x_{i,j}$  represents the  $j$ -th measured quantitative value.

Since the wearable-sensory data is often collected over different time periods (e.g., with different start and end date), the sequence lengths usually vary among different time series (Liu et al. 2016). Also, readings of wearable sensors are usually lost at various unexpected moments because of sensor or communication errors (e.g., power outages) (Manashty, Light, and Soleimani 2018). Hence, the sensory data often exhibits variable-length and missing values.

*Problem Statement.* Given a wearable-sensory time series  $\mathbf{x}_i$  with variable-length and missing values, the objective is to learn the  $d$ -dimensional latent vector  $\mathbf{y}_i \in \mathbb{R}^d$  that captures the unique temporal patterns of time series  $\mathbf{x}_i$ .

## Methodology: *HeartSpace*

*HeartSpace* consists of three components: i) Day-specific time series encoding; ii) Temporal pattern aggregation network; and iii) Siamese-triplet network optimization strategy.

**Time Series Segmentation** Considering that periodicity has been demonstrated as an important factor that governs human sensory data (e.g., heart rate) with time-dependent transition regularities (Nakamura, Takimoto-Inose, and etc

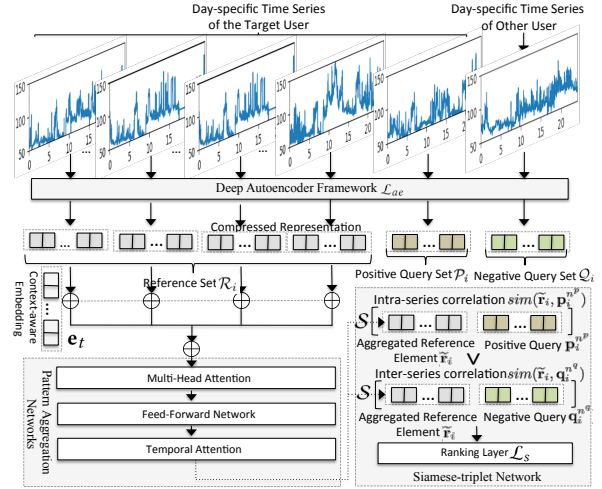


Figure 1: *HeartSpace* Framework. The training flow can be summarized as: (1) partition raw sensory data to a set of day-long time series; (2) map each day-long time series into a representation vector by Day-Specific Time Series Encoding Module (3) fuse day specific representations through Temporal Pattern Aggregation Network (4) update parameters based on reconstruction loss and Siamese-triplet loss.

2018), and the sensed time series data are often variable-length, we first partition the wearable-sensory time series (i.e.,  $\mathbf{x}_i$ ) of each user  $u_i$  into  $T$  (indexed by  $t$ ) separated day-long time series ( $T$  may vary among users).

**Definition 2 Day-long Time Series**  $\mathbf{x}_{i,t}$ . Each  $t$ -th divided day-long time series of  $\mathbf{x}_i$  is denoted as  $\mathbf{x}_{i,t} \in \mathbb{R}^K$ , where  $K = 1440$  is the number of minutes included in one day. In  $\mathbf{x}_{i,t}$ , each element  $x_{i,t}^k$  is the measurement from user  $u_i$  at the  $k$ -th time step in  $\mathbf{x}_{i,t}$ . Due to the data incompleteness issue of the collected time series, we set the element  $x_{i,t}^k$  as 0 to keep equally-spaced intervals for missing measurement.

## Day-Specific Time Series Encoding

To explore the underlying repeated local patterns and reduce dimensions of day-long time series data, we first propose a convolution autoencoder module to map each individual series  $\mathbf{x}_{i,t}$  into a common low-dimensional latent space. In general, the encoder first takes day-long time series as the input and then translates it into a latent representation which encodes the temporal pattern. Then, the decoder network reconstructs the data which is identical with the input  $\mathbf{x}_{i,t}$  in the ideal case. To keep the input dimension consistent with complete day-specific time series, we fill in zero value to missing observations. However, it may bring in the negative effect in the encoding process. Since the filled value are treated equally as other valid inputs when apply kernels in each convolutional layer, the generated features may incorrectly encoded and further lead to the error propagation from low to high layers. To resolve this issue, we propose a dual-stage gating mechanism into a convolution autoencoder module. More specifically, each layer of our deep autoencoder framework is a four-step block: i) convolution network; ii) channel-wise gating mechanism; iii) temporal gating mechanism; and iv) pooling operation. Figure 2 presents the architecture of our deep autoencoder module.

**Convolutional Layers** Firstly, we apply convolutional layers to encode the local pattern of day-long time series  $\mathbf{x}_{i,t}$ . Let's denote  $\mathbf{V}_{i,t}^{l-1}$  as the feature map representation of  $(l-1)$ -th layer. The output of  $l$ -th layer is given as:

$$\mathbf{V}_{i,t}^l = f(\mathbf{W}_c^l * \mathbf{V}_{i,t}^{l-1} + \mathbf{b}_c^l) \quad (1)$$

where  $f(\cdot)$  is the activation function and  $*$  denotes the convolutional operation.  $\mathbf{W}_c^l$  and  $\mathbf{b}_c^l$  represents the transformation matrix and bias term in  $l$ -th layer, respectively.

**Channel-Wise Gating Mechanism** The goal of the channel-wise gating mechanism is to re-weight hidden units by exploiting the cross-channel dependencies and select the most informative elements from the encoded feature representation  $\mathbf{V}_{i,t}^l$  (Hu, Shen, and Sun 2018). To exploit the dependencies over channel dimension, we first apply temporal average pooling operation  $\mathcal{F}_{pool}^{cg}(\cdot)$  on the feature representation  $\mathbf{V}_{i,t}^l$  over temporal dimension ( $1 \leq k \leq K$ ) to produce the summary of each channel-wise representation as:

$$\mathbf{z}_{i,t}^l = \mathcal{F}_{pool}^{cg}(\mathbf{V}_{i,t}^l) = \frac{1}{K} \sum_{k=1}^K \mathbf{V}_{i,t,k}^l \quad (2)$$

where  $\mathbf{z}_{i,t}^l$  is the intermediate representation of  $\mathbf{V}_{i,t}^l$  after average pooling operation over temporal dimension. Then, our channel-wise gating mechanism recalibrates the information distribution among all elements across channels as:

$$\mathbf{a}_{i,t}^l = \text{Sigmoid}(\mathbf{W}_2^{cg} \cdot \text{ReLU}(\mathbf{W}_1^{cg} \cdot \mathbf{z}_{i,t}^l)) \quad (3)$$

where  $\mathbf{a}_{i,t}^l$  denotes the channel-wise importance vector in which each entry is the each channel's importance.  $\mathbf{W}_1^{cg}$  and  $\mathbf{W}_2^{cg}$  are learned parameters of fully connected networks. Finally, the channel-wise representations  $\tilde{\mathbf{V}}_{i,t}^l$  is learned as:

$$\tilde{\mathbf{V}}_{i,t,;,c}^l = \mathbf{V}_{i,t,;,c}^l \mathbf{a}_{i,t,c}^l \quad (4)$$

where  $c$  is the channel index.

**Temporal-wise Gating Mechanism** To re-weight the hidden units by capturing the temporal dependencies of feature representation across time steps, we also apply a gating mechanism on temporal dimension to further learn focus points in the time-ordered internal feature representation  $\tilde{\mathbf{V}}_{i,t}^l$  (output from the channel-wise gating mechanism). Similar to the gating mechanism procedures encoded in Equations 2, 3, and 4, we first apply the channel average pooling operation on feature representation  $\tilde{\mathbf{V}}_{i,t}^l$  over channel dimension and get  $\hat{\mathbf{V}}_{i,t}^l$  as the summarized feature representation which jointly preserve the channel-wise and temporal dependencies.

**Encoder-Decoder Configuration** We present the architecture configuration of our deep autoencoder module.

**Encoder** Given the day-long time series  $\mathbf{x}_{i,t} \in \mathbb{R}^K$ , we use ReLU activation function and contain 5 convolutional layers (*i.e.*, Conv1-Conv5) followed by channel-wise, temporal-wise gating mechanism and pooling layers. Particularly, Conv1-Conv5 is configured with the one-dimensional kernel with  $\{9, 7, 7, 5, 5\}$  and filter sizes with

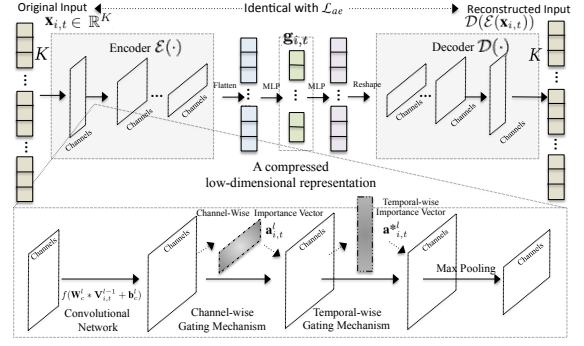


Figure 2: Illustration of Day-Specific Time Series Encoding.

$\{32, 64, 64, 128, 128\}$ , respectively. Then, we perform the flatten operation on the output to generate a one-dimensional feature representation and feed it into a fully connected layer with Tanh activation function to generate the final latent representation  $\mathbf{g}_{i,t}$  corresponding to the time series  $\mathbf{x}_{i,t}$ .

**Decoder** The decoder is symmetric to the encoder in terms of layer structure. First, the representation  $\mathbf{g}_{i,t}$  is uncompressed by a single-layer with Tanh activation function and then followed by a series of five deconvolutional layers with ReLU activation function. The kernel and filter sizes is in reverse order to be symmetric to the encoder architecture configuration. Channel-wise and Temporal-wise are applied in the first four layer after deconvolutional operation.

**Loss Function in Deep Autoencoder Module:** We formally define the reconstruction loss function as below:

$$\mathcal{L}_{ae}^i = \sum_t \|\mathbf{m} \odot (\mathcal{D}(\mathcal{E}(\mathbf{x}_{i,t})) - \mathbf{x}_{i,t})\|_2^2 \quad (5)$$

where  $\mathbf{m} \in \mathbb{R}^K$  is a binary mask vector corresponding to each element in  $\mathbf{x}_{i,t}$ . In particular,  $m^k = 1$  if  $x_{i,t}^k \neq 0$  (*i.e.*, has measurement) and  $m^k = 0$  otherwise.  $\odot$  is the element-wise product operation,  $\mathbf{x}_{i,t}$  is the input,  $\mathcal{E}(\cdot)$  and  $\mathcal{D}(\cdot)$  represents the encoder and decoder function.

### Temporal Pattern Aggregation Network

While applying the autoencoder framework to map day-long time series into a low-dimensional vector, how to appropriately fuse day-specific temporal patterns still remains a significant challenge. To address this challenge, we develop a temporal pattern aggregation network which promotes the collaboration of different day-specific temporal units for conclusive cross-time representations. Figure 3 shows the architecture of our temporal pattern aggregation network which consists of three major modules: i) Context-aware time embedding module; ii) multi-head aggregation network; iii) temporal attention network.

**Context-Aware Time Embedding Module** From the deep autoencoder module, given the time series  $\mathbf{x}_i$  of user  $u_i$ , we learn a set of date-ordered latent representations with size of  $T$ , *i.e.*,  $\mathcal{G}_i = \{\mathbf{g}_{i,1}, \dots, \mathbf{g}_{i,T}\}$ . In reality, different people may exhibit different wearable-sensory data distribution due to specific daily routines (Probst, Pryss, and etc 2016). To incorporate the temporal contextual signals into our learning framework, we further augment our model with a time-aware embedding module, which utilizes the relative

time difference between the last time step and each previous one. For example, given a time series with three date information {2018-10-01, 2018-10-20, 2018-10-25}, we generate a date duration vector as {24, 5, 0} (the day duration between 2018-10-01 and 2018-10-25 is 24 days). To avoid the occurrence of untrained long date duration in testing instances, we adopt timing signal method (Vaswani et al. 2017) to represent a non-trainable date embedding. Formally, the vector  $\mathbf{e}_t$  of  $t$ -th day is derived as:

$$e_{t,2i} = \sin\left(\frac{t}{10000^{2i/d_e}}\right); e_{t,2i+1} = \cos\left(\frac{t}{10000^{2i/d_e}}\right) \quad (6)$$

where  $d_e$  is the embedding dimension ( $2i + 1$  and  $2i$  are the odd and even index in the embedding vector). New context-aware latent vector  $\mathbf{h}_{i,t} \in \mathbb{R}^{d_e}$  is generated by element-wise adding each day-specific feature representation  $\mathbf{g}_{i,t}$  and date embedding  $\mathbf{e}_t$ , to incorporate the temporal contextual signals into the learned embeddings.

**Multi-Head Aggregation Network.** During the pattern fusion process, we develop a multi-head attention mechanism which is integrated with a point-wise feedforward neural network layer, to automatically learn the quantitative relevance in different representation subspaces across all context-aware temporal patterns). Specifically, given the  $i$ -th time series, we feed all context-aware day-specific embeddings  $\mathbf{H}_i = \{\mathbf{h}_{i,0}, \dots, \mathbf{h}_{i,T}\}$  into a multi-head attention mechanism. Here,  $M$ -heads attention conducts the cross-time fusion process for  $Q$  subspaces. Each  $q$ -th attention involves a separate self-attention learning among  $\mathbf{H}_i$  as:

$$\tilde{\mathbf{H}}_i^q = \text{softmax}\left(\frac{\mathbf{W}_1^q \cdot \mathbf{H}_i (\mathbf{W}_2^q \cdot \mathbf{H}_i)^T}{\sqrt{d_q}}\right) \mathbf{W}_3^q \cdot \mathbf{H}_i, \quad (7)$$

where  $\mathbf{W}_1^q, \mathbf{W}_2^q, \mathbf{W}_3^q \in \mathbb{R}^{d_q \times d_e}$  represent the learned parameters of  $q$ -th head attention mechanism, and  $d_q$  is the embedding dimension of  $q$ -th head attention, i.e.,  $d_q = d_e/Q$ . Then, we concatenate each learned embedding vector  $\tilde{\mathbf{H}}_i^q$  from each  $q$ -th head attention, and further capture the cross-head correlations as follows:

$$\tilde{\mathbf{H}}_i = \mathbf{W}_c \cdot \text{concat}(\tilde{\mathbf{H}}_i^1, \dots, \tilde{\mathbf{H}}_i^Q) \quad (8)$$

$\mathbf{W}_c \in \mathbb{R}^{d_e \times d_e}$  models the correlations among head-specific embeddings. Hence, we jointly embed multi-modal dependency units into the space with the fused  $\tilde{\mathbf{H}}_i$  using the multi-head attention network. The advantage of our multi-head attention network lies in the exploration of feature modeling in different representation spaces (Zhang et al. 2018). Then, we further feed the fused embedding  $\tilde{\mathbf{H}}_i^c$  into two fully connected layers, which is defined as follows:

$$\tilde{\mathbf{H}}_i^f = \mathbf{W}_2^f \cdot \text{ReLU}(\mathbf{W}_1^f \cdot \tilde{\mathbf{H}}_i^c + \mathbf{b}_1^f) + \mathbf{b}_2^f, \quad (9)$$

where  $\mathbf{W}_1^f, \mathbf{W}_2^f$  and  $\mathbf{b}_1^f, \mathbf{b}_2^f$  are the weight matrix and bias in the feed-forward layer. In our *HeartSpace* framework, we perform multi-head attention mechanism twice.

**Temporal Attention Network.** To further summarize the temporal relevance, we develop a temporal attention network to learn importance weights across time. Formally, our

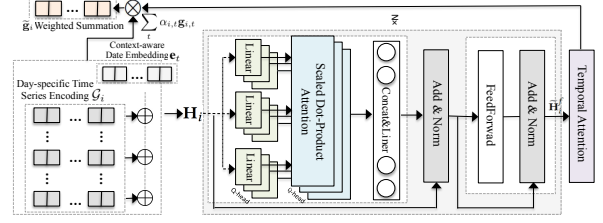


Figure 3: Temporal Pattern Aggregation Network.

temporal attention module can be represented as follows:

$$\alpha_i = \text{softmax}(\mathbf{c} \cdot \text{Tanh}(\mathbf{W}^a \tilde{\mathbf{H}}_i^f + \mathbf{b}^a)); \tilde{\mathbf{g}}_i = \sum_t \alpha_{i,t} \mathbf{g}_{i,t} \quad (10)$$

Output  $\tilde{\mathbf{H}}_i^f$  is first fed into a one fully connected layer and then together with the context vector  $\mathbf{c}$  to generate the importance weights  $\alpha_i$  through the softmax function. The aggregated embedding  $\tilde{\mathbf{g}}_i$  is calculated as a weighted sum of day-specific embeddings based on the learned importance weights. For simplicity, we denote our temporal pattern aggregation network as  $\tilde{\mathbf{g}}_i = \mathcal{A}(\mathcal{G}_i)$ .

### Siamese-triplet Network Optimization Strategy

Our Siamese-triplet network optimization framework aim to enhance the encoded user feature representations with the consideration of constrain, i.e., making representation pairs from same user closer to each other and representation pairs from different user further apart. We first define the following terms to be used in our optimization strategy.

**Definition 3 Reference Set  $\mathcal{R}_i$ :** we define  $\mathcal{R}_i$  to represent the sampled reference set of user  $u_i$ . In particular,  $\mathcal{R}_i = \{\mathbf{r}_i^1, \dots, \mathbf{r}_i^{N^r}\}$ , where  $N^r$  is size of reference set corresponding to  $N^r$  sampled day-specific time series of  $\mathbf{x}_i$  defined in Definition 2. Each entry in  $\mathcal{R}_i$  represents the  $n_r$ -th sampled time series from user  $i$ .

**Definition 4 Positive Query Set  $\mathcal{P}_i$ :** we define  $\mathcal{P}_i = \{\mathbf{p}_i^1, \dots, \mathbf{p}_i^{N^p}\}$  to denote the positive query set of user with size of  $N^p$ . Specifically, every entry  $\mathbf{p}_i^{n^p}$  represents the  $n^p$ -th sampled day-specific time series from user  $u_i$ .

**Definition 5 Negative Query Set  $\mathcal{Q}_i$ :**  $\mathcal{Q}_i = \{\mathbf{q}_i^1, \dots, \mathbf{q}_i^{N^q}\}$  is defined to as the negative query set for user  $u_i$ , which is the sampled  $N^q$  day-specific time series from other users except user  $u_i$ , i.e.,  $u_{i'} (i' \neq i)$ .

Based on the above definitions, given a specific user  $u_i$ , we first aggregate the elements from user  $u_i$ 's reference set  $\mathcal{R}_i$  as:  $\tilde{\mathbf{r}}_i = \mathcal{A}(\mathcal{R}_i)$ , where  $\mathcal{A}(\cdot)$  is the aggregation function which represents the developed temporal pattern aggregation network. Then, we compute the cosine similarity of aggregated reference element  $\tilde{\mathbf{r}}_i$  and each query (i.e.,  $\mathbf{p}_i^{n^p}$  and  $\mathbf{q}_i^{n^q}$ ) from the generated positive query set  $\mathcal{P}_i$  and negative query set  $\mathcal{Q}_i$ . Formally, the similarity estimation function  $\text{sim}$  is presented as follows:

$$\begin{aligned} \text{sim}(\tilde{\mathbf{r}}_i, \mathbf{p}_i^{n^p}) &= \tilde{\mathbf{r}}_i \cdot (\mathcal{E}(\mathbf{p}_i^{n^p}))^T; \quad n^p \in [1, \dots, N^p]; \\ \text{sim}(\tilde{\mathbf{r}}_i, \mathbf{q}_i^{n^q}) &= \tilde{\mathbf{r}}_i \cdot (\mathcal{E}(\mathbf{q}_i^{n^q}))^T; \quad n^q \in [1, \dots, N^q]; \end{aligned} \quad (11)$$

where  $\text{sim}(\tilde{\mathbf{r}}_i, \mathbf{p}_i^{n^p}) \in \mathbb{R}^1$  and  $\text{sim}(\tilde{\mathbf{r}}_i, \mathbf{q}_i^{n^q}) \in \mathbb{R}^1$ . By capturing the temporal consistency of each individual user  $u_i$

and inconsistency among different users, we optimize representations which preserve inherent relationships between each user’s reference set and query set, *i.e.*, time series embeddings from the same user are closer to each other, while embeddings from different users are more differentiated from each other. Therefore, we formally define our loss function as follows:

$$\mathcal{L}_s^i = \sum_{n^p} \sum_{n^q} \max(0, \text{sim}(\tilde{\mathbf{r}}_i, \mathbf{q}_i^{s^q}) - \text{sim}(\tilde{\mathbf{r}}_i, \mathbf{p}_i^{s^p}) + z) \quad (12)$$

where  $z$  is the margin between two similarities. The objective function of joint model is defined as:  $\mathcal{L}_{joint} = \sum_i \mathcal{L}_{ae}^i + \lambda \mathcal{L}_s^i$ , where  $\lambda$  is the coefficient which control the weight of Siamese-triplet loss. The model parameters can be derived by minimizing the loss function. We use Adam optimizer to learn the parameters of *HeartSpace*. The model optimization process is summarized in Algorithm 1.

---

**Algorithm 1:** The Model Inference of *HeartSpace*.

---

**Input:** User set  $\mathcal{U}$ ; reference set size  $N^r$ , positive query size  $N^p$ , negative query size  $N^q$

- 1 Initialize all parameters;
- 2 while not converge do
- 3   sample a set of users from user set  $\mathcal{U}$ ;
- 4   foreach user  $u_i$  do
- 5     sample support set  $\mathcal{R}_i$  and positive set  $\mathcal{P}_i$ ;
- 6     sample negative set  $\mathcal{Q}_i$ ;
- 7     feed each entry in  $\mathcal{R}_i, \mathcal{P}_i$  and  $\mathcal{Q}_i$  into autoencoder to get daily representations and compute  $\mathcal{L}_{ae}^i$ ;
- 8     aggregate support set  $\mathcal{R}_i$  and derive  $\mathcal{L}_s^i$ ;
- 9   end
- 10 update all parameters w.r.t  $\mathcal{L}_{joint} = \sum_i \mathcal{L}_{ae}^i + \mathcal{L}_s^i$ ;
- 11 end

---

**Unsupervised and semi-supervised learning scenarios.** *HeartSpace* is a general representation learning model that is flexible for both unsupervised (without labeled instances) and semi-supervised (limited number of labeled instances) learning. In semi-supervised learning, given the labeled time series and its target value, we take the learned representation vector as the input of a single-layer perceptrons with a combined loss function, *i.e.* integrate the joint objective function  $\mathcal{L}_{joint}$  with the loss function based on cross-entropy (categorical values) or MSE (quantitative values).

## Evaluation

### Experimental Settings

**Data Description.** We evaluate the model performance on two real-world heart rate time series data.

**Garmin Heart Rate Data.** It comes from an on-going research study of workplace performance which measures the physiological states of employees in multiple companies. It is collected from 578 participants (age between 21 to 68) by Garmin band from March 2017 to August 2018. Each measurement is formatted as (user id, heart rate, timestamp).

**Fitbit Heart Rate Data.** We collect this dataset from a research project at a University which aims to collect survey and wearable data from an initial cohort of 698 students

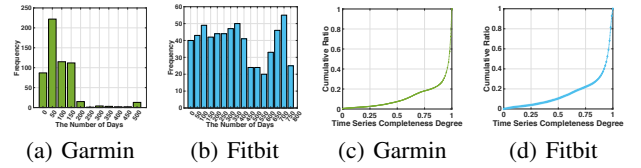


Figure 4: Distribution of Time Series Length (a-b) and Completeness Degree (c-d) on Both Garmin and Fitbit Data.

(age between 17 to 20) who enrolled in the Fall semester of 2015. This dataset is collected by Fitbit Charge during the 2015/2016 and 2016/2017 academic years.

**Data Distribution.** We show the distribution of wearable-sensory time series data in Figure 4 in terms of time series length  $J_i$  and completeness degree (*i.e.*, the ratio of non-zero elements in day-specific time series  $\mathbf{x}_i^J$ ) on Garmin and Fitbit heart rate data. As depicted in Figure 4 (a) and (b), the different datasets have different time series distributions. Furthermore, Figure 4 (c) and (d) reveals that data incompleteness is ubiquitous, *e.g.*, there exists more than 20% day-specific time series with data incompleteness  $< 0.8$ , which poses a further challenge for our *HeartSpace*. These observations are the main motivation to develop a temporal pattern aggregation network and a dual-stage gating mechanism for handling variable-length time series with incomplete data.

**Methods for Comparison.** We compared it with the following representation learning methods:

- **Convolutional Autoencoder (CAE)** (Bascol, Emonet, and etc 2016): CAE is a representation learning framework by applying convolutional autoencoder to map the time series patterns into latent embeddings.
- **Deep Sequence Representation (DSR)** (Amiriparian et al. 2018): DSR is a general-purpose encoder-decoder feature representation model on sequential data with two deep LSTMs, one to map input sequence to vector space and another to map vector to the output sequence.
- **Multi-Level Recurrent Neural Networks (MLR)** (Cheng et al. 2017): MLR is a multi-level feature learning model to extract low- and mid-level features from time series. RNNs with bidirectional-LSTM architectures are employed to learn temporal patterns.
- **Sequence Transformer Networks (STN)** (Oh, Wang, and Wiens 2018): STN is an end-to-end trainable method for learning structural information of clinical time-series data, to capture temporal and magnitude invariances.
- **Wave2Vec** (Yuan, Xun, and others 2019): It is a sequence representation learning framework using skip-gram model by considering sequential contextual signals.
- **DeepHeart** (Bhattacharjee et al. 2018): DeepHeart models the temporal pattern of heart rate time-series data with the integration of the CNN and RNN networks.

**Evaluation Protocols.** We evaluate the accuracy of binary-class classification tasks in terms of *F1-score*, *Accuracy* and *AUC*, and evaluate the classification performance on multi-class in terms of *Macro-F1* and *Micro-F1*. We summarize the details for four different tasks as follows:

Table 1: User identification performance.

Data	Garmin Heart Rate Data						Fitbit Heart Rate Data					
	Feb			Aug			Feb			Aug		
Method	F1-score	Accuracy	AUC	F1-score	Accuracy	AUC	F1-score	Accuracy	AUC	F1-score	Accuracy	AUC
CAE	0.6584	0.6505	0.7112	0.6841	0.6980	0.7705	0.5794	0.5767	0.6023	0.6060	0.5996	0.6387
DSR	0.6496	0.6433	0.6926	0.6948	0.6964	0.7722	0.6478	0.6467	0.6962	0.6136	0.5984	0.6411
MLR	0.6524	0.6379	0.6859	0.7032	0.7046	0.7765	0.6431	0.6395	0.6977	0.6596	0.6497	0.7051
STN	0.6161	0.5727	0.5984	0.7330	0.7406	0.8176	0.7123	0.7186	0.7789	0.7297	0.7276	0.7875
Wave2Vec	0.7431	0.7515	0.8327	0.8246	0.8301	0.9090	0.7785	0.7783	0.8626	0.8136	0.8121	0.8938
DeepHeart	0.7313	0.7384	0.8125	0.7507	0.7567	0.8446	0.6784	0.6805	0.7462	0.7155	0.7143	0.7842
<i>HeartSpace</i>	<b>0.7646</b>	<b>0.7649</b>	<b>0.8410</b>	<b>0.8587</b>	<b>0.8621</b>	<b>0.9352</b>	<b>0.7997</b>	<b>0.7977</b>	<b>0.8696</b>	<b>0.8330</b>	<b>0.8315</b>	<b>0.9147</b>

- User Identification:** For user identification, each method learns a mapping function to encode the day-specific time series data into a low-dimensional representation vector. Then, given multiple day-specific time series data from one user and an unknown day-specific time series, the task is to predict whether the unknown time series is collected from the same user’s multiple day-specific time series.
- User Demographic Inference:** We evaluate whether user demographics, such as gender and age are predictable by using a similar experimental construct as in (Dong et al. 2014). The age information is categorized into four categories (*i.e.*, Young: from 18 to 24, Young-Adult: from 23 to 34, Middle-age: from 39 to 49, senior: from 49 to 100).
- Personality Prediction:** We considered two personality attributes of the participants, namely Conscientiousness and Agreeableness. We considered a classification task of a binary prediction on these attributes — high or low for each participant  $u_i$  (McCrae and John 1992).

### Parameter Settings

We implemented *HeartSpace* framework with Tensorflow. The code will be released once accepted. For fair comparison, all experiments are conducted across all participants in the testing data and the average performance is reported. Furthermore, the validation was run ten times and the average performance numbers are reported. The embedding dimension is 64 and support size is set as 6. The positive and negative sampling size is set as 2 and 4, respectively. Furthermore, the margin value is 1 and the siamese-triplet weight is 0.1. We optimized all methods with Adam with batch size of 64 and learning rate of 0.001. We utilized the Glorot initialization (Glorot and Bengio 2010) and grid search (Grover and Leskovec 2016) strategies for hyperparameter initialization and tuning of all compared methods.

Table 2: User demographic inference results.

Demographic	Age		Gender	
	Micro-F1	Macro-F1	Micro-F1	Macro-F1
CAE	0.5174	0.3644	0.6744	0.6558
DSR	0.5058	0.2590	0.6453	0.6334
MLR	0.5233	0.2704	0.6453	0.6281
STN	0.5291	0.3460	0.6279	0.6228
Wave2Vec	0.5465	0.3540	0.6570	0.6455
DeepHeart	0.4942	0.2664	0.6395	0.6189
<i>HeartSpace</i>	<b>0.5581</b>	<b>0.3773</b>	<b>0.7035</b>	<b>0.6724</b>

### Performance Comparison

**User Identification.** Table 1 shows the user identification performance on both datasets. We can observe that

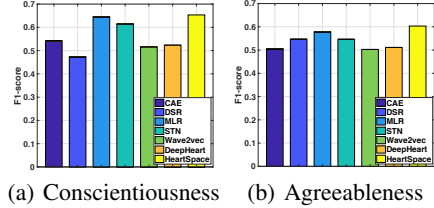


Figure 5: Evaluation results of personality detection.

*HeartSpace* obtains significant improvement over baselines in all cases, which suggests the advantage of *HeartSpace* in capturing the unique signatures of individuals. Although other deep learning methods preserve the temporal structural information of each individual time series, they cannot handle the variable-length and incompleteness of wearable-sensory data, which reveals the practical difficulties in learning accurate models across non-continuous time steps.

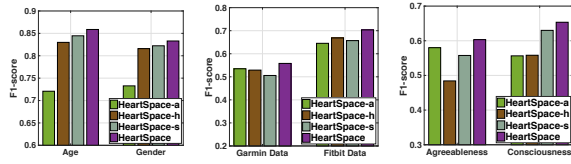
To make thorough evaluation, we compare *HeartSpace* with all baselines across different training and test time periods (*e.g.*, Feb and Aug). We note that the best performance is consistently achieved by *HeartSpace* with different forecasting time periods, which reflects the robustness of *HeartSpace* in learning the latent representations over time.

**Demographic Inference.** The demographic inference performance comparison between *HeartSpace* and other competitive methods on the Garmin heart rate data is shown in Table 2. We can note that our *HeartSpace* outperforms other baselines in inferring users’ age and gender information, which further demonstrate the efficacy of our *HeartSpace* in learning significantly better time series embeddings than existing state-of-the-art methods. Similar results can be observed for the Fitbit heart rate data. In summary, the advantage of *HeartSpace* lies in its proper consideration of comprehensive temporal pattern fusion for time series data.

**Personality Prediction.** Figure 5 shows the personality prediction results on two different categories (*i.e.*, Agreeableness and Conscientiousness). We observe that *HeartSpace* achieves the best performance in all personality cases. The performance is followed by DSR which extracts both multi-level temporal features during the representation learning. This further verifies the utility of temporal pattern fusion in mapping time series data into the latent space.

### Model Ablation Study of *HeartSpace*

We perform ablation experiments over a number of key components of *HeartSpace* to better understand their impacts.



(a) User Identification (b) Demographic (c) Personality  
Figure 6: Evaluation on *HeartSpace* variants.

- **Effect of Siamese-triplet Network *HeartSpace-s*.** A model variant without Siamese-triplet network to model intra- and inter-time series inter-dependencies.
- **Effect of Deep Autoencoder Module. *HeartSpace-a*.** A simplified version of *HeartSpace* without deep autoencoder module, *i.e.*, only consider  $\mathcal{L}_s$  (Siamese-triplet Network) in the loss function.
- **Effect of Multi-head Attention Network. *HeartSpace-h*.** A model variant without the multi-head attention to learn weights of different day-specific temporal patterns.

We report the results in Figure 6. Notice that the full version of *HeartSpace* achieves the best performance in all cases, which suggests: (i) The efficacy of the designed Siamese-triplet network optimization strategy for preserving structural information of implicit intra- and inter-time series correlations. (ii) The effectiveness of *HeartSpace* in capturing complex temporal dependencies across time steps for variable-length sensor data. (iii) The effectiveness of *HeartSpace* in exploring feature modeling in different representation spaces during our pattern fusion process.

### Hyperparameter Studies

Figure 7 shows the hyperparameter study results. We observe that *HeartSpace* is not sensitive to different parameters and could reach high performance under a cost-effective parameter choice, which demonstrates the robustness of *HeartSpace*. Furthermore, we notice that larger hidden dimensionality does not necessarily bring better performance. In addition, we set the dimension size as 64 due to the consideration of the performance and computational cost. We can observe that both the positive query set size and negative query set size, as well as siamese triple loss coefficient have a relatively low impact on the model performance.

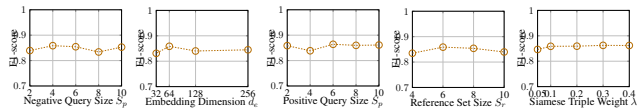
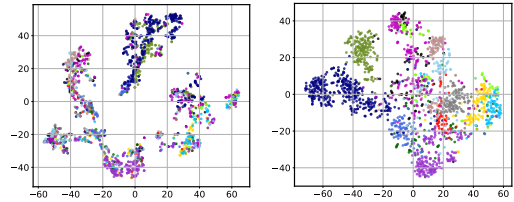


Figure 7: Hyperparameter Studies of *HeartSpace*

### Case Study: Visualization

We further visualize the low-dimensional time series representations learned by *HeartSpace* and one selected baseline (DeepHeart) on Garmin heart rate dataset. Figure 8 shows the 2D t-SNE projections of day-specific time series embeddings from randomly sampled 15 users. We can observe that the embeddings from the same user could be identified by our *HeartSpace* and cluster them closer than other embeddings (more accurate feature representations), while the embeddings learned by DeepHeart of different users are mixed and cannot be well identified.



(a) DeepHeart (b) *HeartSpace*

Figure 8: Embedding Visualizations of *HeartSpace* v.s. DeepHeart. Each color corresponds to one specific user.

### Related Work

**Deep Learning for Healthcare Applications.** With the advent of deep learning techniques, many deep neural network frameworks have been proposed to address various challenges in healthcare informatics (Bai et al. 2018; Ma, Gao, and others 2018; Cao et al. 2017; Suhara, Xu, and Pentland 2017; Choi, Bahadori, and others 2017). For example, Cao *et al.* (Cao et al. 2017) proposed an end-to-end deep architecture for the prediction of human mood. Bai *et al.* (Bai et al. 2018) modeled sequential patient data and predict future clinical events. This work furthers this direction of investigation by proposing a general time series representation learning framework to capture hierarchical structural correlations exhibited from human heart rate data, which cannot be handled by previous models.

**Representation Learning on wearable-sensory Data.** A handful of studies (Ballinger et al. 2018; Amiriparian et al. 2018; Lehman et al. 2018) have investigated the representation learning on wearable-sensory data. Ballinger *et al.* (Ballinger et al. 2018) proposed a semi-supervised learning method to detect health conditions. Amiriparian *et al.* (Amiriparian et al. 2018) explored the deep feature representations to aid the diagnosis of cardiovascular disorders with sequence to sequence autoencoders. While these pioneering studies have demonstrated the effectiveness of representation learning on wearable-sensory data, they do not address our problem of designing a unified model that dynamically captures the evolving temporal characteristics from wearable-sensory time series with variable-length.

### Conclusion

This work presented *HeartSpace*, a wearable-sensory time series representation learning framework that addresses several challenges stemming from such data and also overcomes the limitations of current state-of-the-art approaches, including dealing with incomplete and variable length time series, intra-sensor / individual variability, and absence of ground truth. *HeartSpace* first learns latent representation to encode temporal patterns of individual day-specific time series with a deep autoencoder model. Then, an integrative framework of a pattern aggregation network and a Siamese-triplet network optimization maps variable-length wearable-sensory time series into the common latent space such that the implicit intra-series and inter-series correlations well preserved. Extensive experiments demonstrate that the latent feature representations learned by *HeartSpace* are significantly more accurate and generalizable than baselines.

## References

- [Amiriparian et al. 2018] Amiriparian, S.; Schmitt, M.; Cummins, N.; Qian, K.; Dong, F.; and Schuller, B. 2018. Deep unsupervised representation learning for abnormal heart sound classification. In *EMBC*, 4776–4779. IEEE.
- [Bai et al. 2018] Bai, T.; Zhang, S.; Egleston, B. L.; and Vucetic, S. 2018. Interpretable representation learning for healthcare via capturing disease progression through time. In *KDD*, 43–51. ACM.
- [Ballinger et al. 2018] Ballinger, B.; Hsieh, J.; Singh, A.; et al. 2018. Deepheart: Semi-supervised sequence learning for cardiovascular risk prediction. In *IJCAI*.
- [Bascol, Emonet, and etc 2016] Bascol, K.; Emonet, R.; and etc. 2016. Unsupervised interpretable pattern discovery in time series using autoencoders. In *SSPR*, 427–438. Springer.
- [Bhattacharjee et al. 2018] Bhattacharjee, T.; Datta, S.; Das, D.; Choudhury, A. D.; Pal, A.; and Ghosh, P. K. 2018. A heart rate driven kalman filter for continuous arousal trend monitoring. In *EMBC*, 3572–3577. IEEE.
- [Cao et al. 2017] Cao, B.; Zheng, L.; Zhang, C.; Yu, P. S.; Piscitello, A.; Zulueta, J.; Ajilore, O.; Ryan, K.; and Leow, A. D. 2017. Deepmood: modeling mobile phone typing dynamics for mood detection. In *KDD*, 747–755. ACM.
- [Cheng et al. 2017] Cheng, M.; Sori, W. J.; Jiang, F.; Khan, A.; and Liu, S. 2017. Recurrent neural network based classification of ecg signal features for obstruction of sleep apnea detection. In *CSE*, volume 2, 199–202. IEEE.
- [Choi, Bahadori, and others 2017] Choi, E.; Bahadori, M. T.; et al. 2017. Gram: graph-based attention model for healthcare representation learning. In *KDD*, 787–795. ACM.
- [Dong et al. 2014] Dong, Y.; Yang, Y.; Tang, J.; and etc. 2014. Inferring user demographics and social strategies in mobile social networks. In *KDD*, 15–24. ACM.
- [Glorot and Bengio 2010] Glorot, X., and Bengio, Y. 2010. Understanding the difficulty of training deep feedforward neural networks. In *AISTATS*, 249–256.
- [Grover and Leskovec 2016] Grover, A., and Leskovec, J. 2016. node2vec: Scalable feature learning for networks. In *KDD*, 855–864. ACM.
- [Hu, Shen, and Sun 2018] Hu, J.; Shen, L.; and Sun, G. 2018. Squeeze-and-excitation networks. In *CVPR*, 7132–7141.
- [Lehman et al. 2018] Lehman, E. P.; Krishnan, R. G.; Zhao, X.; Mark, R. G.; and Li-wei, H. L. 2018. Representation learning approaches to detect false arrhythmia alarms from ecg dynamics. In *MLHC*, 571–586.
- [Liu et al. 2015] Liu, B.; Li, J.; Chen, C.; and etc. 2015. Efficient motif discovery for large-scale time series in healthcare. *TII* 11(3):583–590.
- [Liu et al. 2016] Liu, X.; Liu, L.; Simske, S. J.; and etc. 2016. Human daily activity recognition for healthcare using wearable and visual sensing data. In *ICHI*, 24–31. IEEE.
- [Ma, Gao, and others 2018] Ma, F.; Gao, J.; et al. 2018. Risk prediction on electronic health records with prior medical knowledge. In *KDD*, 1910–1919. ACM.
- [Manashty, Light, and Soleimani 2018] Manashty, A.; Light, J.; and Soleimani, H. 2018. A concise temporal data representation model for prediction in biomedical wearable devices. *Internet of Things Journal*.
- [McCrae and John 1992] McCrae, R. R., and John, O. P. 1992. An introduction to the five-factor model and its applications. *Journal of personality* 60(2):175–215.
- [Nakamura, Takimoto-Inose, and etc 2018] Nakamura, K.; Takimoto-Inose, A.; and etc. 2018. Cross-modal perception of human emotion in domestic horses. *Scientific Reports* 8(1):8660.
- [Ni, Muhlstein, and McAuley 2019] Ni, J.; Muhlstein, L.; and McAuley, J. 2019. Modeling heart rate and activity data for personalized fitness recommendation.
- [Oh, Wang, and Wiens 2018] Oh, J.; Wang, J.; and Wiens, J. 2018. Learning to exploit invariances in clinical time-series data using sequence transformer networks. *Machine Learning for Healthcare*.
- [Op De Beéck, Meert, and others 2018] Op De Beéck, T.; Meert, W.; et al. 2018. Fatigue prediction in outdoor runners via machine learning and sensor fusion. In *KDD*, 606–615. ACM.
- [Probst, Pryss, and etc 2016] Probst, T.; Pryss, R.; and etc. 2016. Emotional states as mediators between tinnitus loudness and tinnitus distress in daily life: Results from the track-your-tinnitus application. *Scientific Reports* 6:20382.
- [Suhara, Xu, and Pentland 2017] Suhara, Y.; Xu, Y.; and Pentland, A. 2017. Deepmood: Forecasting depressed mood based on self-reported histories via recurrent neural networks. In *WWW*, 715–724. ACM.
- [Sun, Leng, and etc 2015] Sun, Y.; Leng, B.; and etc. 2015. A novel wavelet-svm short-time passenger flow prediction in beijing subway system. *Neurocomputing* 166:109–121.
- [Vaswani et al. 2017] Vaswani, A.; Shazeer, N.; Parmar, N.; Uszkoreit, J.; and etc. 2017. Attention is all you need. In *NIPS*, 5998–6008.
- [Wang et al. 2018] Wang, J.; Zhang, J.; Bao, W.; and etc. 2018. Not just privacy: Improving performance of private deep learning in mobile cloud. In *KDD*, 2407–2416. ACM.
- [Yuan, Xun, and others 2019] Yuan, Y.; Xun, G.; et al. 2019. Wave2vec: Deep representation learning for clinical temporal data. *Neurocomputing* 324:31–42.
- [Zhang et al. 2018] Zhang, J.; Shi, X.; Xie, J.; and etc. 2018. Gaan: Gated attention networks for learning on large and spatiotemporal graphs.
- [Zhu et al. 2018] Zhu, Y.; Yeh, C.-C. M.; Zimmerman, Z.; and etc. 2018. Matrix profile xi: Scrimp++: Time series motif discovery at interactive speeds. In *ICDM*, 837–846. IEEE.